NASTRAN Structural Model for the Large 64-Meter Antenna Pedestal, Part II — Improved Model

C. T. Chian

Ground Antennas and Facilities Engineering Section

Static analysis and a computer structural model for the large 64-m antenna pedestal are developed using the MSC version of the NASTRAN program. This improved pedestal model includes the haunch areas and the actual pressure pattern of the oil under the hydrostatic bearing pad. The results obtained from the new improved model have indicated that the deflections due to pad loads are in good agreement with field measurements. The top surface deflection of the pedestal obtained from the NASTRAN model is used as an input to the oil film computer program to determine the minimum oil film thickness under the pad.

I. Introduction

This article is the second in a series of reports on the static analysis and computer modeling performed for the large 64-m antenna pedestal. The pedestal is under pressure loadings at the three hydrostatic bearing pads. The pedestal computer model previously reported in Ref. 1 has been improved in order to better represent the displacement and force distribution throughout the pedestal, as well as to obtain the state of stress and strain.

The deflections of the pedestal under the pad resulted from the NASTRAN model are used as inputs to the oil film height program[1] to evaluate the corner oil film thickness between the pad and the runner. A minimum hydrostatic bearing oil film of

0.13 mm (0.005 in.) is required to avoid any metal to metal contact between the pad and the runner and to accommodate any runner malfunctioning and placement tolerance.

II. Description of the Improved Model

The first computer structural model of the pedestal was reported in Ref. 1. The assumptions made in this initial model are that (1) the pedestal is a cylinder of uniform wall thickness, thus ignoring the effect of the haunch; (2) the pedestal loading is uniform with 6.9×10^6 N/m² (1000 psi) pressure over the pad length and width; and (3) the modulus of elasticity of the entire pedestal concrete is 2.8×10^{10} N/m² (4.0×10^6 psi). By symmetry, the pedestal could be modelled as one 60 degree segment with two boundary conditions: (1) zero slope at the points representing the centerline of the pad, and

---

(2) zero slope at the points representing midposition between two pads.

In the present improved pedestal model, the first two assumptions are modified to include (1) the actual haunch contour in the pedestal to provide additional stiffness on the pedestal wall, and (2) the actual pressure profile of the oil under the pad. The model was developed using the MSC version of the NASTRAN structural program.

The improved pedestal model consists of a wall, haunch, and top slab, as shown in Fig. 1. Figure 2 is a cross-sectional diagram of the pedestal. A cross-sectional diagram of the hydrostatic bearing is shown in Fig. 3. Deflected shapes of the hydrostatic bearing pad and runner surface are illustrated in Fig. 4. Relative deflections within the hydrostatic bearing pad and within the runner surface from centerline to edge of pad are shown as Δ_p and Δ_r, respectively. Design constraints required that the mismatch of deflected surfaces, δ, be within 0.10 mm (0.004 in.). Part of this 0.10 mm (0.004 in.) total mismatch, a maximum mismatch of deflected shapes of 0.08 mm (0.003 in.) was established as the limit for creep during construction, hence before the bearing pads could be moved. The remaining 0.025 mm (0.001 in.) was the design criteria for mismatch of elastic deformations (Ref. 2). If the creep strains are compensated for by releveling of the runner, then the total δ of 0.10 mm (0.004 in.) might be tolerated for the elastic deformations portion alone.

The actual pressure profile of the oil under the hydrostatic bearing pad is illustrated in Fig. 5. For simplicity, the pressure pattern of the oil under the pad is assumed to be symmetric with respect to the pad centerline in the NASTRAN pedestal model. Therefore, $p_1 = p_3$ and $p_4 = p_6$. Pad 3, which experiences the highest load among the three pads, is the one considered in our model. The values of the pad recess pressures are given in Table 1.

Figure 6 shows a typical deflection map of the top pedestal surface under pad load. This deflection map is used as the input to the oil film height model to determine the minimum oil film thickness between the pad and the runner.

III. Comparison with Field Measurements

Field-measured load-deformation relationships of the pedestal were obtained and used to calibrate the present NASTRAN pedestal model. The pad load tests can also be used to determine the spatial distribution of deteriorated concrete in the haunch.

The field measurements were conducted by JPL in cooperation with Construction Technology Laboratories (CTL) of Skokie, Illinois. (CTL is a division of the Portland Cement Association.) Figure 7 shows the locations of the gauges for deflection measurements. Instruments were installed to measure vertical deformations over a 1.27 m (50 in.) gauge length on the external surface of the haunch and the wall. Figure 8 is a schematic of the instrumentation used. As shown, small blocks were bonded to the structure at the preselected locations. A direct current differential transformer (DCDT) mounted in a fixture was attached to the upper block. A wire from the spring-loaded plunger of the DCDT was attached to the lower block. The output of the DCDT was continuously recorded during the time required for antenna Pad 3 to be moved across the instrumented location. This time is approximately 3 minutes.

Figures 9 and 10 show the good correlation between the field deflection measurements and the NASTRAN predicted values for two different locations: azimuth 49° and azimuth 96°.

IV. Conclusions

The improved NASTRAN structural model for the large 64-m antenna pedestal shows excellent correlation with the field deflection measurement. This new model incorporates improvements over the previous model of Ref. 1 which includes the actual haunch areas in the pedestal and the actual pressure pattern of the oil under the hydrostatic bearing pad.

The maximum pad out-of-flatness and the minimum oil film thickness are important factors to evaluate the condition of the hydrostatic bearing performance. The new pedestal computer model will be a useful tool in the large antenna bearing rehabilitation and upgrade studies. A series of parametric studies using the improved NASTRAN pedestal model and the oil film thickness program will be performed. For example, the effects of varying moduli of elasticity in different regions of the pedestal concrete, and the effects of increasing pad loads due to 64-m to 70-m extension will be investigated.

Acknowledgment

References

1. Chain, C. T., Katow, M. S., and McGinness, H., "NASTRAN Structural Model for the Large 64-m Antenna Pedestal, Part I," *TDA Progress Report 42-74*, Jet Propulsion Laboratory, Pasadena, CA, August 15, 1983.

2. TDA Technical Staff, "The NASA/JPL 64-Meter-Diameter Antenna at Goldstone, California: Project Report," *JPL Technical Memorandum 33-671*, Jet Propulsion Laboratory, Pasadena, CA, July 15, 1974.

3. Hinkle, J. G., Castelli, V., Rippel, H. C., and Zimmerman, C. D., "A Computer Proram for Hydrostatic Bearings Including Effects on Non-Uniform Film Thickness and Relative Velocity for Various Methods of Lubricant Supply," The Franklin Institute, *Final Technical Report F-B2099*, Philadelphia, PA, April, 1964.

Table 1. Pad 3 recess pressures[a]

Recess pressure	p_1	p_2	p_4	p_5
N/m^2	11,383,000	7,757,000	10,859,000	9,480,000
psi	1651	1125	1575	1375

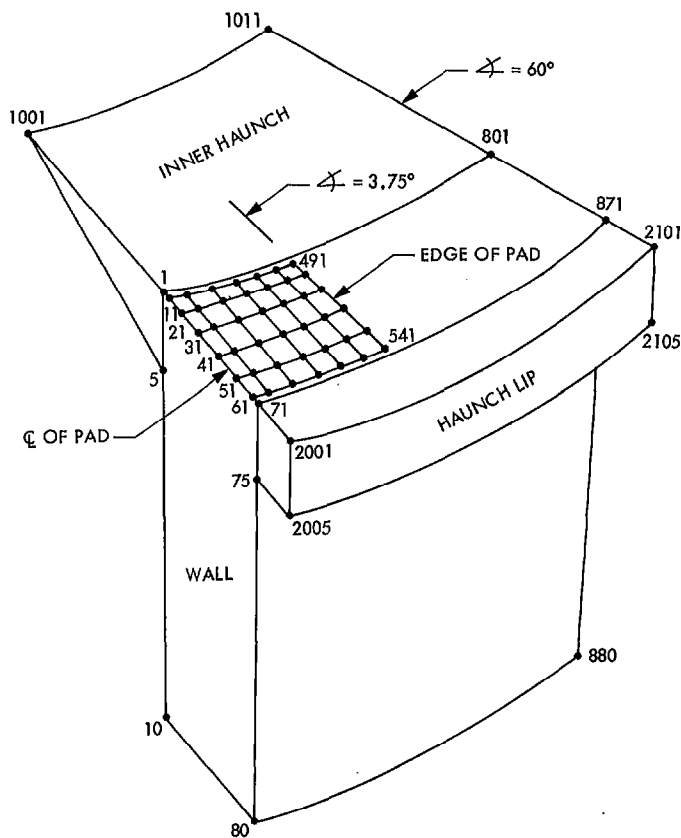[a]Assume $p_1 = p_3 = \frac{1}{2}(p_1 + p_3)$ and $p_4 = p_6 = \frac{1}{2}(p_4 + p_6)$.

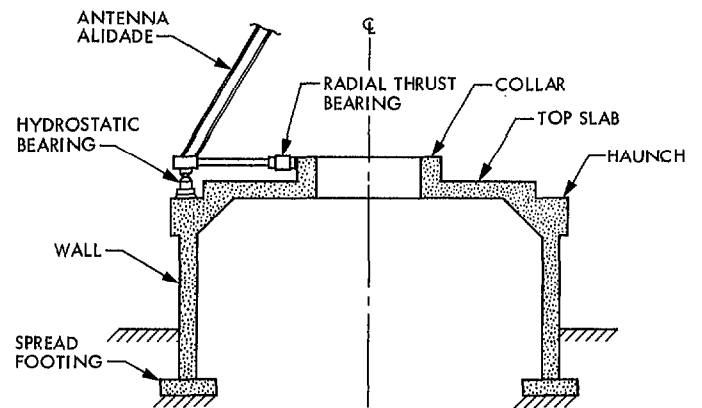Fig. 1. New NASTRAN pedestal model and nodal points
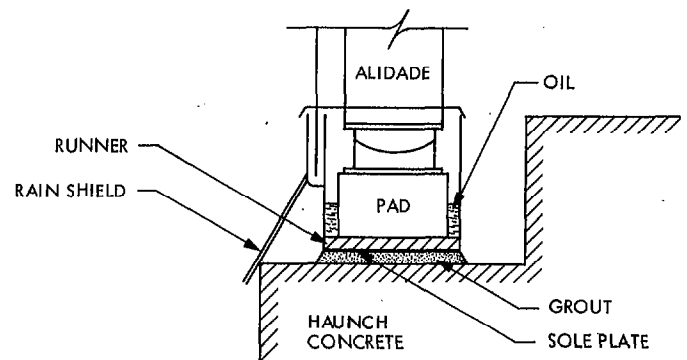
Fig. 2. Cross section of concrete pedestal
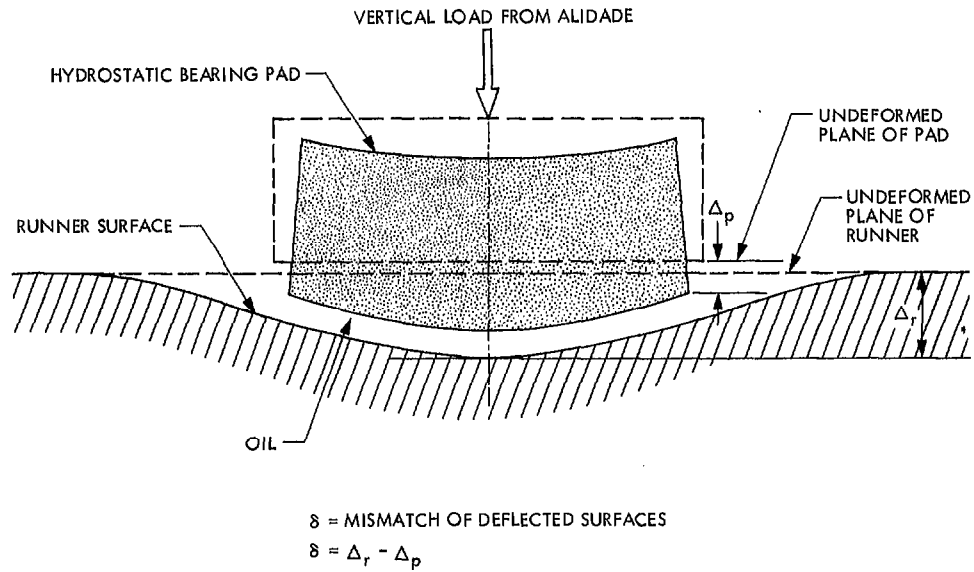
Fig. 3. Cross section of hydrostatic bearing system

VERTICAL LOAD FROM ALIDADE

HYDROSTATIC BEARING PAD

UNDEFORMED PLANE OF PAD

UNDEFORMED PLANE OF RUNNER

RUNNER SURFACE

OIL

δ = MISMATCH OF DEFLECTED SURFACES

$\delta = \Delta_r - \Delta_p$

Fig. 4. Deflections of hydrostatic bearing pad and runner surface

DIMENSIONS IN MILLIMETERS (INCHES)
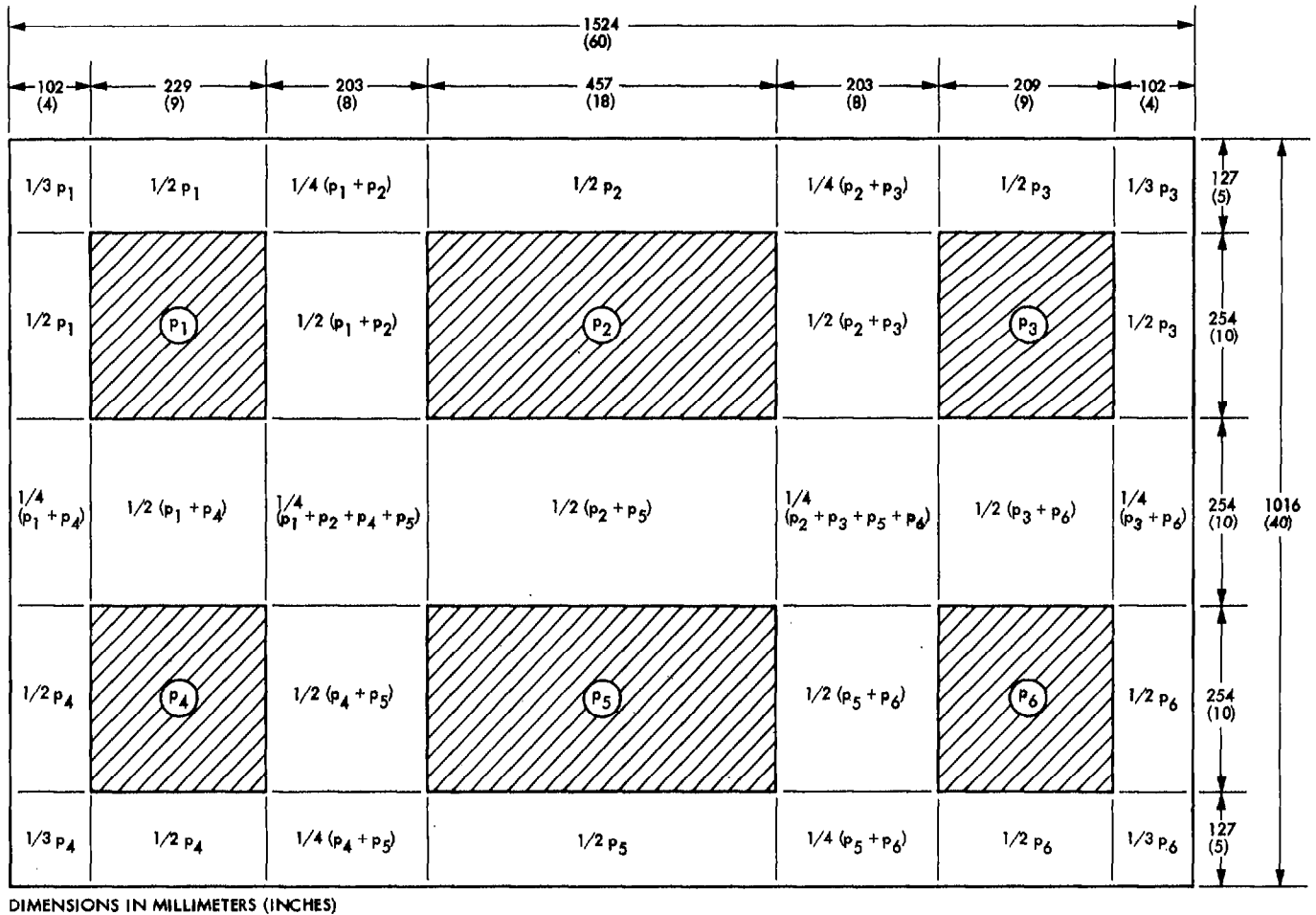
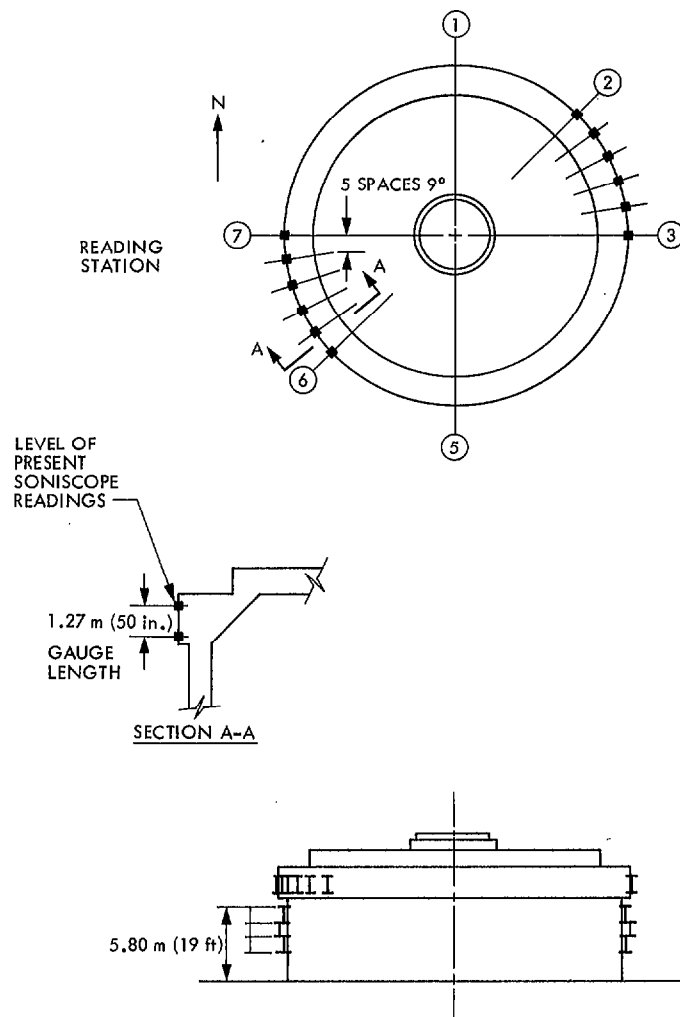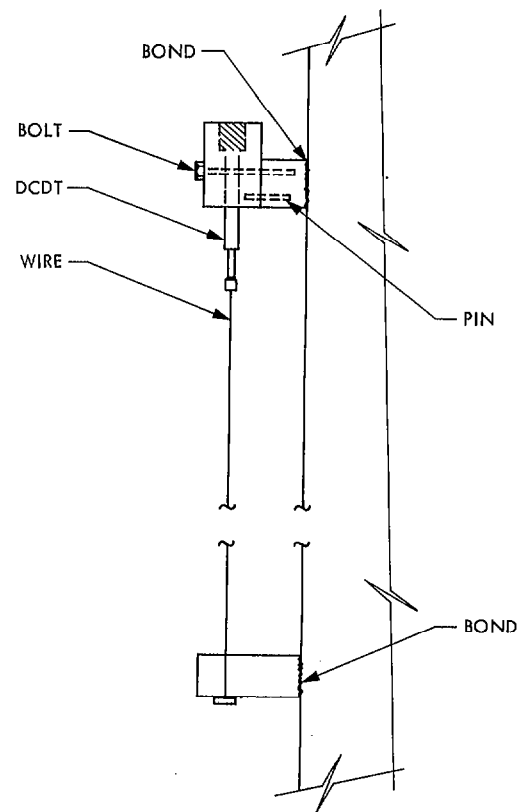Fig. 5. Pressure profile of hydrostatic bearing pad

110
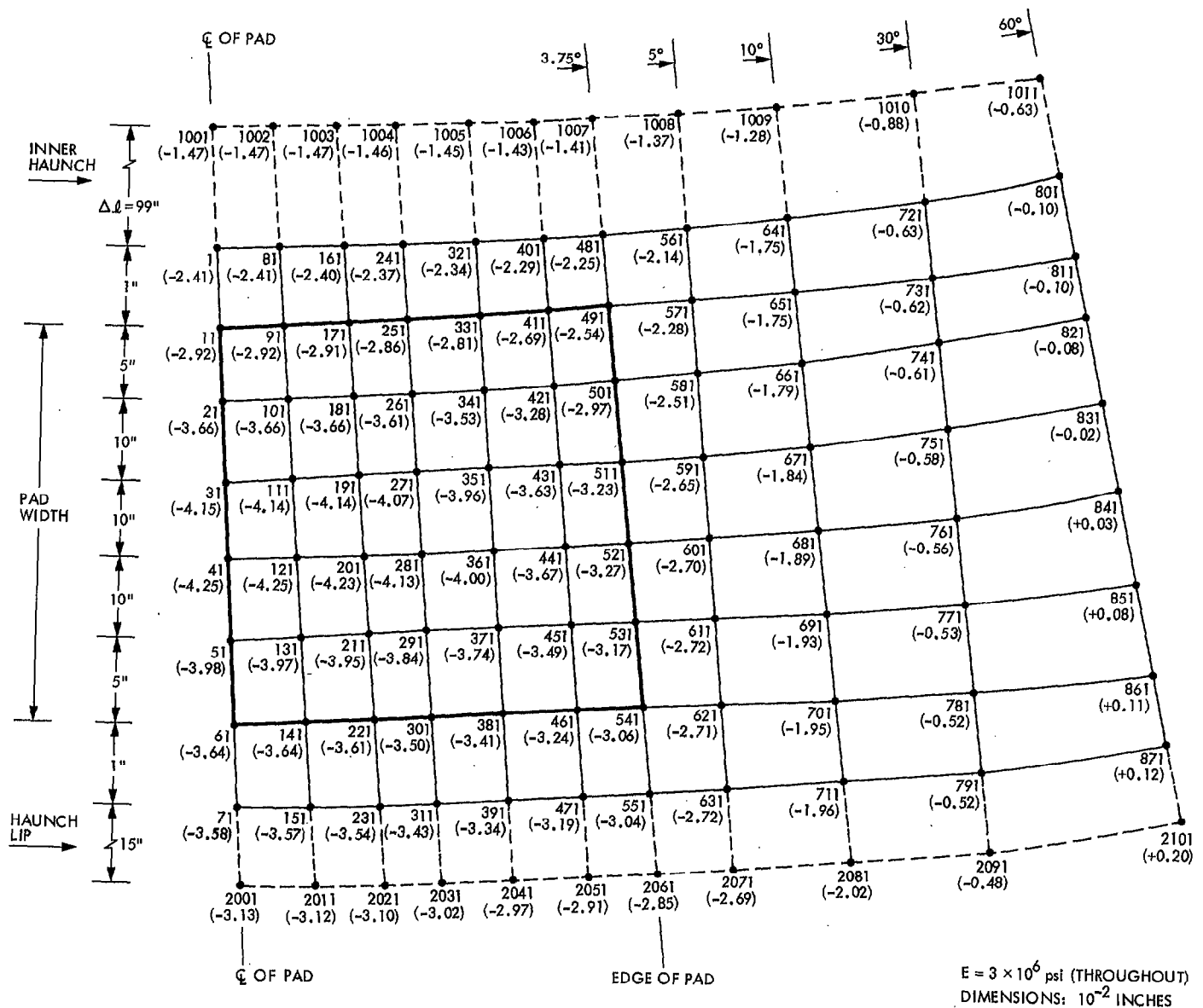
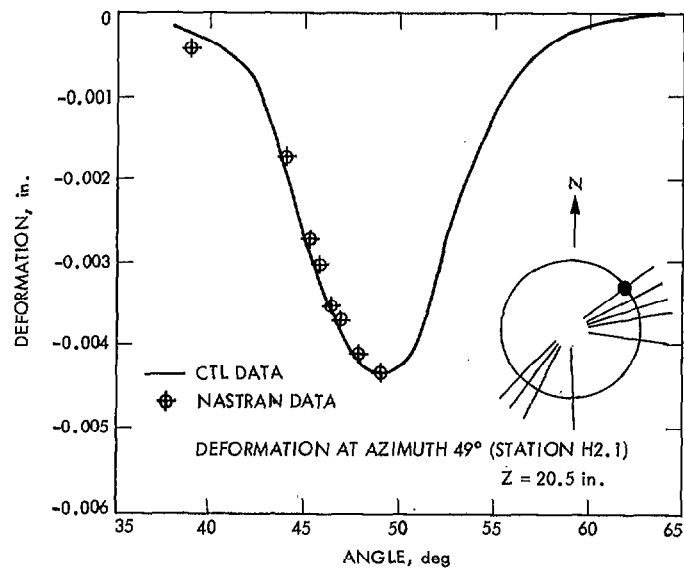**Fig. 6. Deflection map of top pedestal surface**
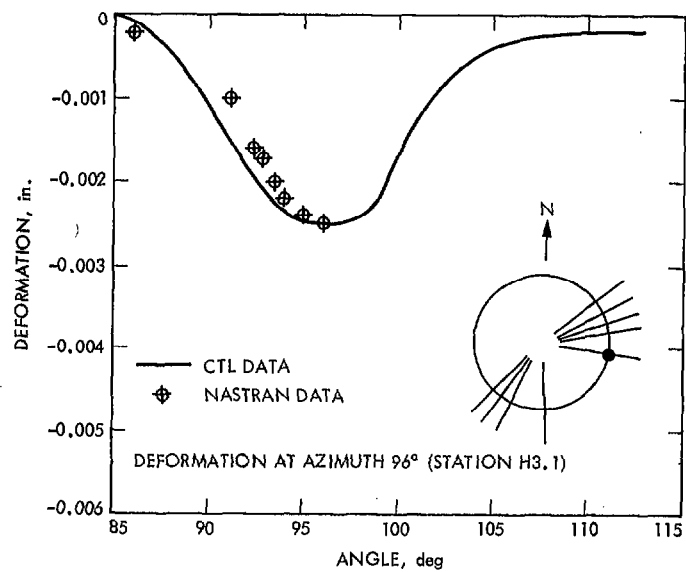
Fig. 7. Location of pad load tests

Fig. 8. Load test instrumentation

Fig. 9. Comparison of the NASTRAN model results with field test data, azimuth = 49°

Fig. 10. Comparison of the NASTRAN model results with field test data, azimuth = 96°